geosciences

MDPI

Article

Hydrogeochemical Characteristics and Isotopic Tools Used to Identify the Mineralization Processes of Bottled Mineral Water in Morocco

Mohammad Ghalit [1], Mohamed Bouaissa [1], Elkhadir Gharibi [1], Jean-Denis Taupin [2,*] and Nicolas Patris [2]

[1] Laboratory of Applied Chemistry and Environment, Team Solid Mineral Chemistry, Faculty of Sciences, Mohammed First University, Oujda, BP 717, Oujda 60000, Morocco
[2] HydroSciences, Faculty of Pharmaceutical and Biological Sciences of Montpellier, IRD, CNRS, CEDEX 05, 34093 Montpellier, France
* Correspondence: jean-denis.taupin@umontpellier.fr

Abstract: Bottled waters are among the most important products in the human diet. In Morocco, eleven bottled mineral waters were analyzed (physicochemical composition and water stable isotopes) to identify their geologic origins and hydrochemical characteristics. The study of the ionic ratios shows that the mechanisms of water–rock interaction, such as the dissolution of carbonate and silicate minerals, influence the chemistry of these mineral waters, which are controlled by lithology and tectonics, sometimes with the influence of deep flux through fractures. The water from the Oulmes plateau shows a Na-HCO_3 chemical facies in relationship with alkaline granite. Moreover, the carbonated waters (EM_G and EM_{GL}) are characterized by high concentrations of Si, Li, Rb, Sr, and Cs due to deep CO_2 flux origin. The waters of Saiss, Middle Atlas, and Rif are of the Ca-HCO_3 type linked mainly to carbonate formation. The stable isotope contents of water range from −7.74 to −5.35‰ for $\delta^{18}O$ and −45.4 to −30.4‰ for δD. The recharge altitude of the aquifer was estimated to be between 250 and 1200 m, following a $\delta^{18}O$ altitudinal gradient between 0.25 and 0.27‰ per 100 m. The industrial production process and the natural presence or artificial addition of CO_2 can also influence the isotopic composition of water. These results can be a relevant guide to decision makers for better exploitation and assessment of the water quality.

Keywords: hydrogeochemical; water origin; stable isotopes; bottled mineral water; Morocco

check for updates

Citation: Ghalit, M.; Bouaissa, M.; Gharibi, E.; Taupin, J.-D.; Patris, N. Hydrogeochemical Characteristics and Isotopic Tools Used to Identify the Mineralization Processes of Bottled Mineral Water in Morocco. *Geosciences* **2023**, *13*, 38. https://doi.org/10.3390/geosciences13020038

Academic Editors: Stefan Geyer and Jesus Martinez-Frias

Received: 28 November 2022
Revised: 12 January 2023
Accepted: 23 January 2023
Published: 29 January 2023

Copyright: © 2023 by the authors. Licensee MDPI, Basel, Switzerland. This article is an open access article distributed under the terms and conditions of the Creative Commons Attribution (CC BY) license (https://creativecommons.org/licenses/by/4.0/).

1. Introduction

In recent years, with the change in lifestyle, people pay more and more attention to the quality of drinking water and its impact on health [1]. The Moroccan water law "36-15" [2], in particular, "Section 2: Water uses" and "Sub-section 3: Exploitation and sale of natural mineral waters, spring waters and table water", define natural mineral water as water that comes from aquifers, and which has a naturally constant chemical composition and does not require any chemical treatment to make it drinkable. Spring water is a natural aquifer water that does not require any chemical treatment to be drinkable.

In many countries, there are regulations specifically governing the sale of bottled mineral water. In the European Community, Directives 1980/777/EEC [3], 1996/70/EC [4], and 2003/40/EC [5] stipulate that bottled water must be groundwater and clearly distinct from ordinary drinking water by its nature.

The quality of groundwater sold in large quantities in bottles is susceptible to the overexploitation of sources. Reasonable and sustainable exploitation is only possible with an in-depth knowledge of the complex dynamics that locally characterize the hydrological cycle [6]. Indeed, the chemistry of water is generally controlled by different factors, such as climatic conditions, interaction with atmospheric gases, hydrolysis, and dissolution of minerals present in dust, soils, and rocks, interactions between dissolved minerals and

organic matter, rate of infiltration through the soil, residence time in the aquifer, mixing with other water, etc. [7–9].

Concentrations of major ions are used to identify the influence of water–rock interactions on the chemistry of the water and to identify the nature of the chemical reactions that take place [10,11].

Stable isotopes of the water molecule are widely used in such assessments [12], in particular for understanding the origins of groundwater from isotopes of precipitation as an input function, recharge zones, and surface–underground interactions [13]. Isotopic signals from rainwater (δ^2H, $\delta^{18}O$) are transferred to groundwater during recharge. For much groundwater, the isotopic composition is equal to the composition of seasonal precipitation [14]. However, unlike in temperate regions, the isotopic composition of groundwater in arid regions can be significantly altered with respect to local precipitation [15]. The cause is the strong isotopic enrichment in heavy isotopes caused by evaporation during storage at the surface before infiltration into the aquifer [13]. In addition, in Morocco, the presence of a mountain system can modify the isotopic content of water which has infiltrated at higher elevations than at the altitudinal level of surface sources or wells with an apparent depletion effect [16].

Bottled waters, sold on the market, can be considered representative samples of their originating aquifers. This enables monitoring over time to show the stability of the chemistry of these waters and the possible impact on quality from human activity.

Over the past two decades, numerous studies worldwide have been carried out to characterize the composition and chemical origin of bottled water [17–20]. The main objective of this study is to consider bottled waters as reliable and chemically stable samples taken from several aquifers with different geological characteristics. This comparative study aims at understanding the origin and the processes that have contributed to the mineralization of bottled water in Morocco. In addition, the isotopic characterization of these waters makes it possible to determine the modes and altitudes of recharge of each aquifer used for the production of bottled water in Morocco.

2. Material and Methods

2.1. Study Area

Morocco is a country located in northwest Africa, it is bordered by the Atlantic Ocean to the west and the Mediterranean Sea to the north, as well as by the country of Mauritania to the south and the country of Algeria to the east (Figure 1a).

The topography of the country is dominated by four mountain ranges; these divide the country into three distinct geographical regions, the mountainous interior, which contains fertile valleys and plateaus, the Rif mountain range in the north of the country which is parallel with the Mediterranean Sea coast, and the three Atlas mountain ranges south of the Rif Mountains (Figure 1c). In the case of the northern and northwestern parts, where the study area is located, the climates are characterized by humid Mediterranean and Atlantic climates (Figure 1b,d). The northwest of the country is the rainiest region with average annual precipitation exceeding 1000 mm, at the level of the High and Middle Atlas as well as in the north of the Rif, while precipitation does not exceed 200 mm in the majority of the other regions of the country (Figure 1e) [21].

This study focuses on seven still natural mineral waters (EM_1 to EM_7): a carbogazeous natural mineral water (EM_G), an artificially carbonated natural mineral water (EM_{GF}), a light carbogazeous natural mineral water (EM_{GL}), and a spring water (ES) (Table 1).

Natural mineral waters and spring waters EM_7 and ES are collected from the Rif region; EM_1, EM_{GF}, and EM_3 are extracted from the South Rif or Pre-Rif corridor; EM_2, EM_4, EM_G, and EM_{GL} are produced from the Oulmes plateau; finally, EM_5 and EM_6 originate from the Middle Atlas (Figure 2) [22]. However, EM_{GL} corresponds to the same water as EM_G with a smaller quantity of gas obtained through partial decarbonation, and EM_{GF} corresponds to the same source as EM_1, to which CO_2 has been artificially added.

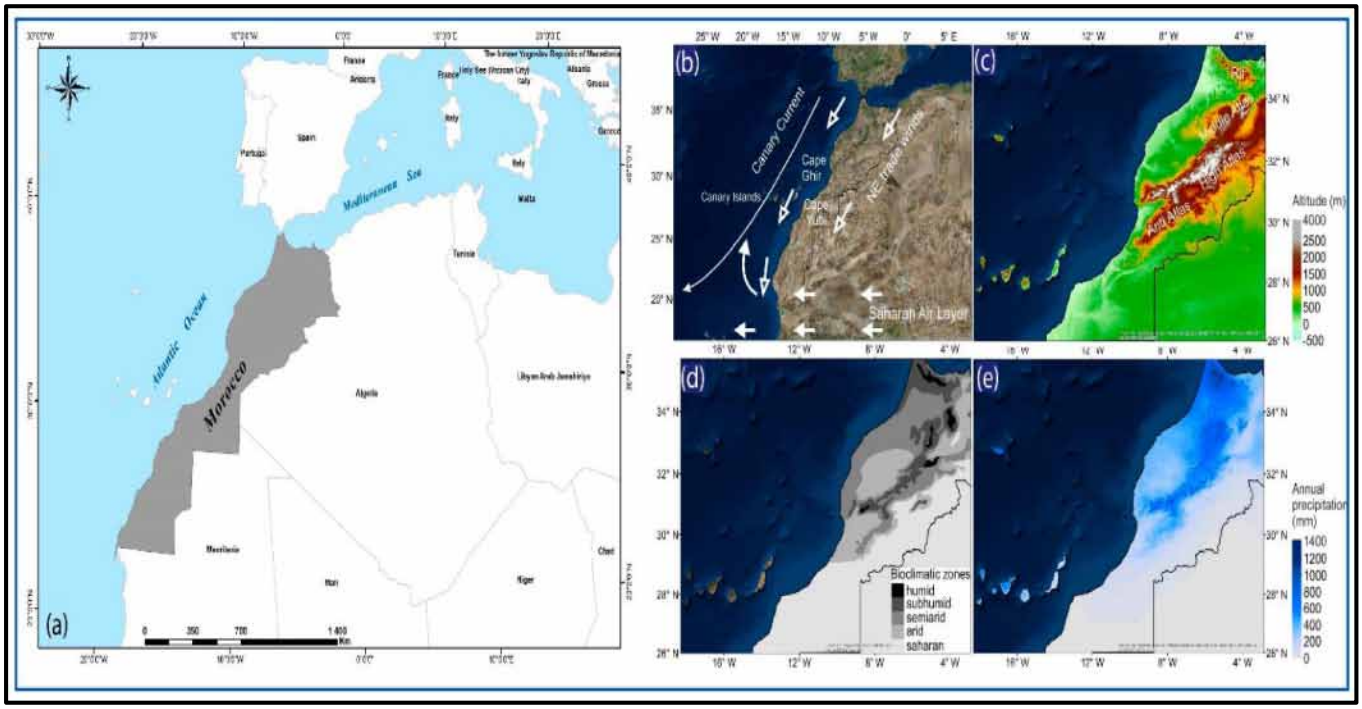

Figure 1. (**a**) Geographical location of Morocco; (**b**) major atmospheric systems and the Canary Current; (**c**) the regional topography; (**d**) distribution of bioclimatic zones; (**e**) distribution of annual precipitation [21].

Table 1. Types of bottled water studied.

Water Type	Name	City	Origin	Depths Below the Ground Surface (m)	Geology
EM_1	Ain Saiss	Fez	Middle Atlas	750	Jurassic carbonate formation (limestone and dolomite)
EM_2	Sidi Ali	Oulmes	Oulmes Plateau	13.8	Granite
EM_3	Sidi Harazem	Fez	Middle Atlas	90	Miocene detrital marls of the Pre-Rif deposited on the Jurassic carbonates of the Atlas
EM_4	Ain Atlas	Oulmes	Oulmes Plateau	-	Granite
EM_5	Ain Ifrane	Ifrane	Middle Atlas	-	Jurassic carbonate formation (limestone and dolomite)
EM_6	Ain Soultane	Ain Soultane	Middle Atlas	-	Jurassic carbonate formation (limestone and dolomite)
EM_7	Chaouen	Chefchaoen	Rif	65	Limestone ridge of the internal Riffian domain
EM_G	Oulmes	Oulmes	Oulmes Plateau	-	Granite
EM_{GF}	Ain Saiss Finely	Fez	Middle Atlas	750	Jurassic carbonate formation (limestone and dolomite)
EM_{GL}	Oulmes Light	Oulmes	Oulmes Plateau	-	Granite
ES	Rif	Chefchaoen	Rif	35	limestone ridge of the internal Riffian domain

From a geological point of view, the Oulmes plateau comprises two main types of geological formations, a granite formation surrounded by an andalusite and biotite schist zone. In the east of these schist formations, there is a quartzite formation outcrop with argillaceous shales containing limestone nodules, sandstones, and limestone [23]. The granitic facies of the Massif of Oulmes, can be classified into two large groups: medium-grained granites with two types of mica, and fine granites [24].

The plain of Sidi Harazem, which contains the aquifer of the EM_3 sample, is formed by terrigenous fluvial type deposits of Plio-Quaternary age, present mainly in the northern part of the plain; this formation is reported under the name of "Conglomerates of Tghaytia" [25].

These conglomerates are unconformity deposits on the sandy marls of the Lower and Middle Pliocene. The formation is made up of a succession of beds of metric conglomerates interspersed by small passes of coarse sandstone marking a set of sequences separated by gully surfaces [26]. The constituent elements of the conglomerates are heterogeneous and polymeric of Liasic or Miocene origin and are fixed in a sandstone and sandstone–clay matrix [27].

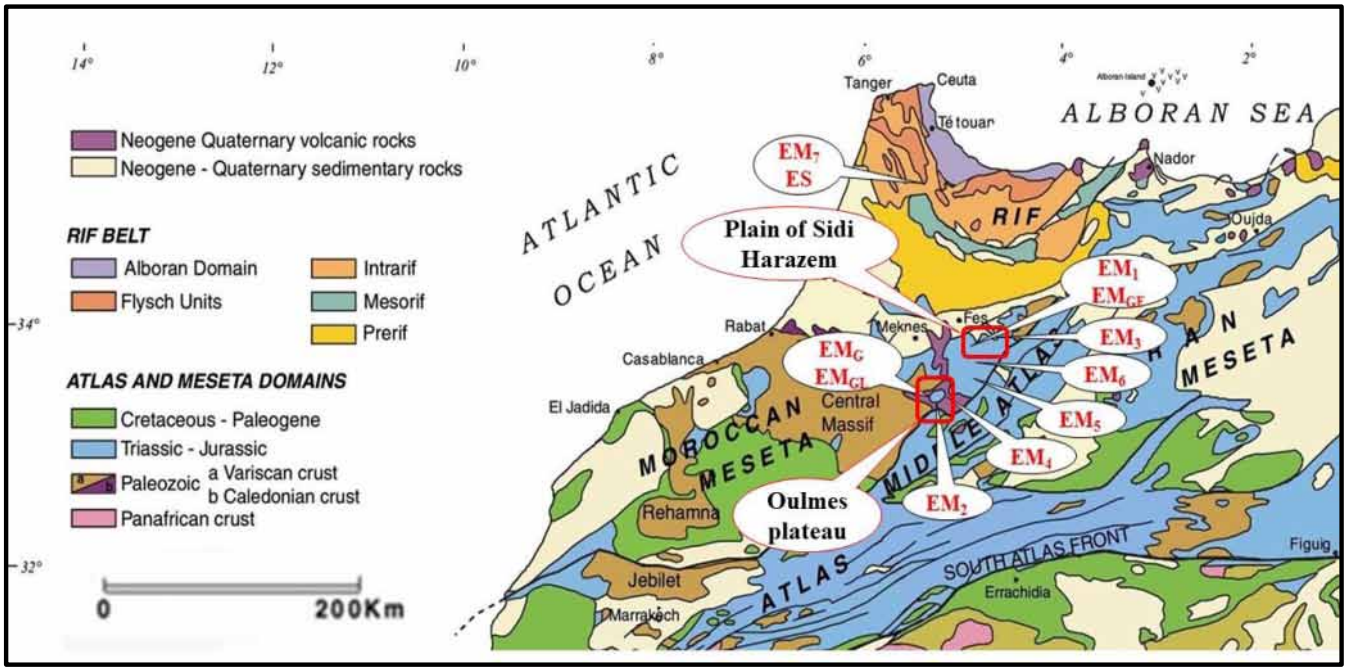

Figure 2. Geological map of the study area and the location of samples [22].

The sources of mineral water, Ain Ifrane (EM_5) and Ain Soultane (EM_6), spring up in the chain of the Middle Atlas, which presents a resistant Jurassic carbonate formation (limestone and dolomite) in which levels of marl, clays, and sandstone are added [28]. These lands are deposited on a Triassic volcano-detrital series formed mainly of clays, sandstones, and alkaline basalts. The waters of the Middle Atlas generally exhibit a strongly calc-magnesian bicarbonate chemism in relation to the geological formations in place. The Triassic salt domes, which are widespread over a large area, outcrop locally (for example in Tissa, 47 km north of Fez), and are also present at different depths in the Pre-Rif Corridor [29].

The Chaouen water (EM_7) is taken from the Ain Sahel Kharrouba source, which emerges at a break in the slope of an unconfined aquifer sitting in Villafranchian alluvium. The supply basin is made up of Quaternary alluvial formations fed by precipitation at the foot of the mountain of the dolomitic limestone ridge of the western Rif. The latter is highly fractured with Jurassic carbonates in which marl levels are interspersed [30]. The marls are of Cenomanian and Senonian age.

The Rif water (ES) is extracted from a shallow water table flowing in an alternating system of shale and sandstone. This water table is recharged at the level of the internal limestone ridge.

2.2. Sampling and Analytical Techniques

Bottled waters are considered chemically stable groundwater samples. In order to support this assumption, physicochemical analyses were carried out over several periods, for 3 years and for 3 different samples in terms of production date (Table S1) to verify the physicochemical stability of these waters. The analyses were carried out on 0.5 L and 1.5 L PET bottles, which were purchased in a supermarket.

The measurements of pH and EC were analyzed under the same temperature at the Laboratory of Applied Chemistry and Environment in the Faculty of Sciences, Oujda. The

hydrogen potential (pH) and electrical conductivity (EC) were determined by using a HI9033 conductivity meter, and a HI98115 pH meter. The major ion analyses were carried out in accordance with the standard methods for the examination of water and wastewater by the American Public Health Association [31]. The bicarbonates (HCO_3^-) and chlorides (Cl^-) were determined by assay method using hydrochloric acid and silver nitrate (0.1 N). Other elements such as nitrates (NO_3^-), sulfates (SO_4^{2-}), phosphates (PO_4^{3-}), ammonium (NH_4^+), and nitrites (NO_2^-) were determined by the colorimetric assay method using a UV-VIS spectrophotometer (Rayleigh UV—9200 (precision ±1 nm)). The analyses of cations and trace elements, 12 parameters in total (Ca^{2+}, Mg^{2+}, Na^+, K^+, P, Si, B, Li, Ba, Rb, Sr, and Cs) were determined by using an ICP-MS model iCAP Q ThermoScientific at the Laboratory of Chemistry, Hydrosciences, Montpellier, France. The stable isotope analyses ($\delta^{18}O$ and δ^2H) were performed on an Elementar Isoprime IRMS at the LAMA Laboratory of HydroSciences, Montpellier. The analysis of $\delta^{18}O$ was carried out by the dual inlet method with an AQUAPREP automaton using equilibration with CO_2 (error ±0.05‰), and the analysis of δ^2H by the continuous flow method using a Eurovector PYROH Elemental Analyzer, through pyrolysis of the water in the presence of chromium under a helium flow (error ±0.8‰).

3. Results and Discussion

3.1. Water Quality

The results of chemical analyses for the 11 types of bottled water studied are given in Table 2. However, Table S2 gives the standard deviation of the results. For the major elements, the results that we found are no different from those identified on the bottle labels. Label data for certain types of water show the chemical stability of water for decades.

Table 2. Average analytical results for bottled water in Morocco.

Water Type	pH	EC	TDS	Na^+	K^+	Mg^{2+}	Ca^{2+}	NH_4^+	P	Cl^-	SO_4^{2-}	HCO_3^-	NO_3^-	NO_2^-
		µS/cm							mg/L					
EM_1	7.50	663	381	15.5	0.47	36.4	63.2	0.003	0.007	42.6	5.14	366.0	8.04	0.004
EM_2	7.55	291	213	21.2	1.92	8.87	18.2	<DL	0.008	16.0	32.1	91.50	0.05	0.002
EM_3	7.44	1299	750	121.9	2.47	36.8	72.4	<DL	0.003	244.9	20.1	341.6	4.50	0.025
EM_4	7.73	335	277	35.5	5.68	10.1	18.2	<DL	0.083	12.4	12.6	158.6	8.34	0.003
EM_5	7.55	582	358	2.54	0.70	37.9	70.1	<DL	0.023	8.88	6.57	420.9	7.15	0.010
EM_6	7.58	695	440	3.23	0.63	44.4	75.2	0.055	0.008	10.6	10.0	420.9	22.5	0.005
EM_7	7.32	518	345	10.9	0.36	13.1	79.8	<DL	0.004	19.5	27.0	256.2	1.58	0.009
EM_G	6.02	2160	1343	230.7	23.4	39.7	112.8	<DL	<DL	289.3	9.68	799.1	2.27	0.068
EM_{GF}	5.45	653	376	14.9	0.46	35.7	61.8	<DL	0.009	47.9	4.66	335.5	8.02	0.004
EM_{GL}	5.71	2160	1318	231.6	23.9	47.8	126.6	0.010	0.003	292.9	10.3	841.8	2.74	0.035
ES	7.78	175	157	6.41	0.35	6.85	29.9	<DL	0.002	10.6	13.4	109.8	0.78	<DL
DL	0.1	0.1	0.1	0.0002	0.001	0.0001	0.0001	0.001	0.0003	0.1	0.02	0.1	0.01	0.001
WHO	6.5–8	-	-	-	-	-	-	-	-	250	250	-	50	3
MS	6.5–8.5	2700	-	-	-	-	-	0.5	-	750	400	-	50	0.5

Water type	Si	B	Li	Ba	Rb	Sr	Cs
				µg/L			
EM_1	2845	8.38	0.46	12.1	0.34	43.7	0.08
EM_2	19,911	16.1	74.8	29.5	6.85	197.6	1.65
EM_3	5240	41.1	87.5	18.3	6.05	499.9	2.17
EM_4	17,824	62.7	28.5	47.3	18.3	314.0	0.10
EM_5	8408	4.16	0.31	5.80	1.86	72.8	0.01
EM_6	2555	7.31	0.68	8.30	0.26	36.1	0.02
EM_7	4275	31.4	1.39	25.5	0.17	257.0	0.00
EM_G	74,898	545.5	3956.4	260.5	323.6	641.6	205.8
EM_{GF}	2707	8.48	0.55	12.2	0.31	41.0	0.08
EM_{GL}	75,674	589.6	4339.9	269.9	327.2	645.4	211.3
ES	4070	14.8	0.59	13.7	0.24	117.5	0.00
DL	78.8456	0.1027	0.0034	0.0022	0.0048	0.0012	0.0002
WHO	-	500	-	700	-	-	-
MS	-	300	-	700	-	-	-

DL: detection limit; WHO: World Health Organization (WHO) guideline values for drinking water [32]; MS: Moroccan food water standards [33].

The low pHs of EM_G and EM_{GL} are due to the dissolution of naturally occurring CO_2 or artificially injected CO_2 in EM_{GF} waters. Based on the information on the label, CO_2 was more likely to be artificially injected during the manufacturing process.

The EC of the samples showed great variability in the range of 175 to 2160 $\mu S.cm^{-1}$. Some samples (EM_3, EM_G, and EM_{GL}) showed extremely high EC (Table 2), which may be attributable to their thermal origin [34–36].

There are few details about the land use in the study zone. In the Moroccan ley, the catchments have a protective perimeter with a minimum distance of 35 m. All catchments are affected by agricultural activities more or less, but there are no urban activities. The Middle Atlas shows the greatest impact of intensive agriculture.

The concentration of nitrate is generally higher in the water withdrawn from the Middle Atlas where there are major agricultural activities. However, the concentration is higher for EM_6 (22.5 mg/L) but remains below the guide value (50 mg/L). On the contrary, on the Oulmes plateau and in the Rif, agriculture activities are sparse and limited, allowing a limited impact. In the Rif (EM7 and ES), the catchments are located in the bottom of gullies, without agriculture activities for 3 km, providing a poor anthropic impact with very low nitrate contents.

The concentration of Ba (Table 2) is generally low because it is either adsorbed on clay minerals or precipitates with sulfate and carbonate in nature [37]. The solubility of Ba compounds increases with decreasing pH, and the highest Ba concentrations in bottled water are expected in low pH water derived from granite rocks for waters of Oulmes origin (EM_2, EM_4, EM_G, and EM_{GL}). Ba concentration depends not only on pH but also on the type of rocks, it can be found in igneous rocks such as granite, at high content levels [38]. Ba is also an alkaline earth metal, and probably has a higher content in the case of alkaline granite (EM_2, EM_4).

Higher concentrations of K, Si, Li, Rb, Sr, and Cs indicate that the water source is in granite rocks [39]. The increase in Li, Rb, and Cs content is associated with CO_2 –Na waters [40]. The concentrations of K, Si, Li, Rb, Sr, and Cs for the waters of Oulmes origin (EM_2, EM_4, EM_G, and EM_{GL}) coming from granitic rocks are much higher than the water coming from other rocks type except EM_3 in marls, which, like EM_G and EM_{GL}, are thermal waters marked with a higher EC. This condition can facilitate the solubility of minerals in the water. However, compared with EM_2, Ba and Rb, two trace elements that are abundant in granitic rocks, show lower content and are probably lower in marls, limiting their presence in the water.

Table 3 shows the matrix of correlation coefficients between the different chemical parameters of the samples studied. This correlation shows that the mineralization of bottled waters in Morocco is mainly controlled by Cl^-, Na^+, Ca^{2+}, Mg^{2+}, HCO_3^-, and K^+, suggesting that the mineralization is controlled by the dissolution/precipitation of rocks.

The hydrochemical facies of bottled water in Morocco were established using the Piper diagram [41] (Figure 3). The results obtained by the projection of the data show that the bottled waters from the Rif, Saiss, and Middle Atlas (EM_1, EM_5, EM_6, EM_7, EM_{GF}, ES) show a Ca-HCO_3 or Ca/Mg-HCO_3 chemical facies, the bottled waters from Oulmes (EM_2, EM_4, and EM_G-EM_{GL}) show, respectively, a Ca/Na(Mg)-HCO_3 and a Na(Ca-Mg)-HCO_3 facies and the carbogazeous waters a Na(Ca)-HCO_3(Cl) facies, and the bottled water from Sidi Hrazem (EM_3) shows a Na(Ca-Mg)-Cl(HCO_3) chemical facies. The original waters of the Oulmes plateau emerge successively in alkaline granites (granite and granite arena) [24], which explains their sodium bicarbonate facies. These waters show high concentrations of Na^+ and K^+, which may be related to the hydrolysis of feldspars such as albite and those contained in granite.

For EM_1/EM_{GF}, EM_5, and EM_6 mineral waters, the calc-magnesian bicarbonate facies are linked to the emergence of springs in the carbonate Jurassic formed by limestones and dolomites.

Table 3. Correlation coefficient matrix between the different chemical parameters of bottled water in Morocco. The bolded values ≥ 0.6 correspond to strong and representative relationship between 2 parameters.

Variables	TDS	Na^+	K^+	Mg^{2+}	Ca^{2+}	NH_4^+	PO_4^{2-}	Cl^-	SO_4^{2-}	HCO_3^-	NO_3^-
TDS	**1**										
Na^+	**0.97**	**1**									
K^+	**0.92**	**0.94**	**1**								
Mg^{2+}	**0.65**	0.48	0.41	**1**							
Ca^{2+}	**0.86**	**0.73**	**0.69**	**0.78**	**1**						
NH_4^+	0.02	−0.12	−0.07	0.41	0.19	**1**					
PO_4^{2-}	−0.31	−0.23	−0.10	−0.35	−0.49	−0.11	**1**				
Cl^-	**0.95**	**0.97**	**0.83**	0.55	**0.74**	−0.13	−0.34	**1**			
SO_4^{2-}	−0.22	−0.10	−0.18	**−0.61**	−0.32	−0.18	−0.11	−0.10	**1**		
HCO_3^-	**0.93**	**0.83**	**0.84**	**0.81**	**0.93**	0.17	−0.32	**0.79**	−0.45	**1**	
NO_3^-	−0.16	−0.32	−0.27	0.45	0.03	**0.85**	0.20	−0.30	−0.46	0.05	**1**

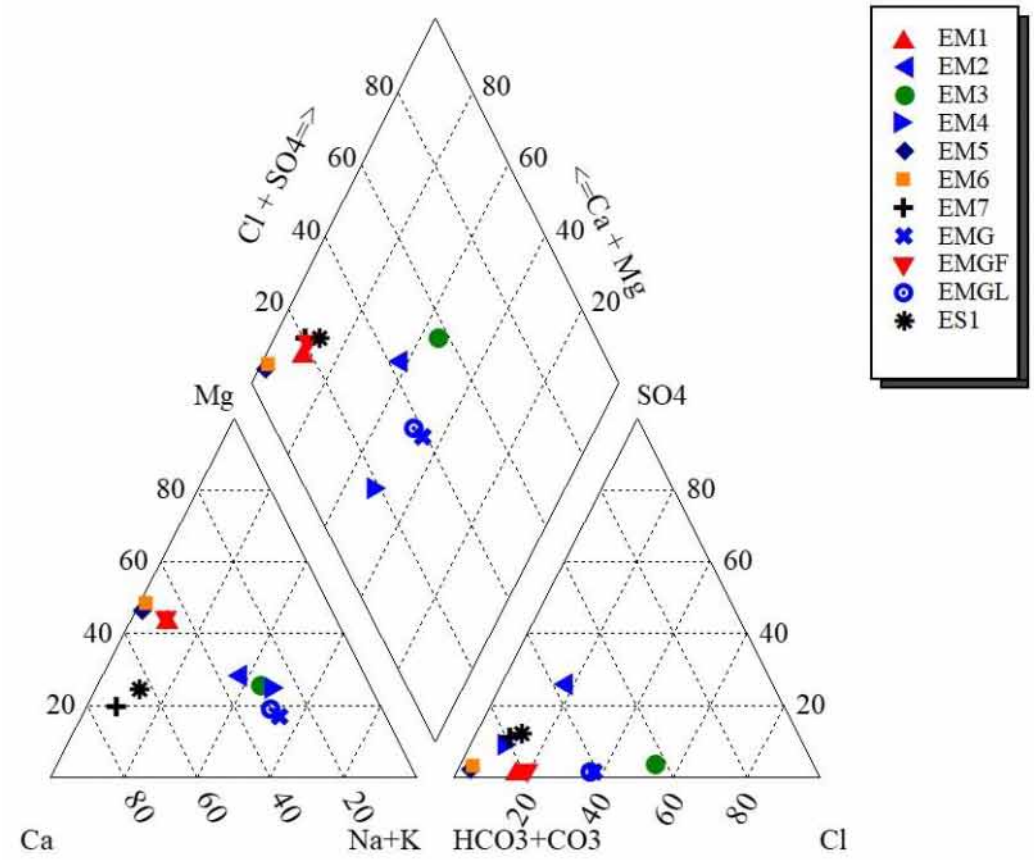

Figure 3. Piper diagram of bottled mineral water in Morocco.

The EM_3 mineral water exhibits a sodium chloride facies, which is related to the contact of the detrital Miocene marls of the Pre-Rif deposited on the Jurassic carbonates of the Atlas. However, the evaporate layers are found in the Miocene marl, which provides Na^+ and Cl^- ions.

The mineralization of EM_7 mineral water and ES spring water is mainly due to calcium bicarbonate, which may come from the limestone ridge of the Inner Rif region.

3.2. Water Mineralization Process

3.2.1. Water–Rock Interaction

Scatter plots, or binary correlation diagrams between ionic elements, make it possible to evaluate and understand the different processes involved in mineralization [42].

The correlation between Cl^- and Na^+ (Figure 4a) shows the presence of three distinct groups. The first group is characterized by Na^+/Cl^- ratios close to 1 (EM_5, EM_6, EM_7, and ES), linked to the dissolution of halite. These waters belong to carbonate formation, this input of halite could be linked with the dissolution of soil salts (Na^+ and Cl^-) that accumulate during the dry season and are removed during the wet season until the aquifer. The second group is characterized by Na^+/Cl^- ratios >1 (EM_2, EM_4, EM_G, and EM_{GL}), and these waters are relatively rich in sodium, suggesting for this element an origin from the geological formation of the Oulmes plateau. Indeed, besides the contribution from rains and the dissolution of halite in soils during the wet seasons, these waters reside in alkaline granites, which constitute a second source of Na^+ ions. Another possibility for the origin of Na^+ ions is a cation exchange between the smectites or phyllosilicates resulting from the degradation of granite by circulating groundwater. The third group, with a Na^+/Cl^- ratio <1 showing a sodium depletion with respect to chlorine, characterizes the waters extracted from Sidi Harazem (EM_3), which pervade heterogeneous conglomerates fixed in a sandstone and sandstone–clay matrix.

The variations of geochemical mechanisms in the aquifer system can also be interpreted from different scatter plots. This allows hypotheses to be made on the origin of these cations, which normally pair up in the aqueous phase, generally in the bicarbonate or sulfated form.

The correlation between (Ca^{2+}+Mg^{2+}) and (HCO_3^-+SO_4^{2-}) (Figure 4b), shows that most of the points are distributed on the line of slope 1, with the exception of the two samples EMG and EMGL, which are thermal waters and naturally carbonated which explains their excess in carbonates. Note that the sulfate contribution always remains very minor (Table 1), except for EM_2, compared with bicarbonates, and this is the reason why Figure 4c shows a similar data distribution pattern. The still natural mineral waters (EM_2 and EM_4) and the carbogazeous natural mineral water (EM_G and EM_{GL}) from Oulmes are slightly above the equilibrium and richer in HCO_3^- ions. This can be related to the alkaline facies of granites where the hydrolysis process produces bicarbonate associated with high sodium concentrations. The relatively high concentration of sulfates in EM_2 could be linked to the hydrolysis of the pyrite, which may be present in granitic fractures. Since these concentrations in EM_4, EM_G, and EM_{GL} plot below the line, there may be a relationship to the dissolution of excess CO_2 gas in the aquifer.

The relation between Ca^{2+} and Mg^{2+} shows that the groundwater extracted from the Rif (EM_7 and ES) and Pre-Rif (EM_3) highlights the relationship between the dissolution of calcite, or dolomite, and the geological structure of the aquifer (Figure 4d). Regarding our results, most of the points are close to the line (Ca^{2+}/Mg^{2+} = 1) indicating the phenomenon of dissolution of the dominant dolomite, while the samples from the Rif (EM_7 and ES), whose ratio is greater than 2, show dissolution of the dominant calcite. For EM_7 water in carbonate formation, Mg^{2+} shows a lower content with respect to Ca^{2+}. The first explanation is mainly an interaction with a calcic formation containing few Mg^{2+}, and a part of the excess of Ca^{2+} could also be linked with sulfates (dissolution of gypsum) which are non-negligible in EM_7. This is shown in Figure 4, which shows a good equilibrium between (Ca^{2+}+Mg^{2+}) and (HCO_3^-+SO_4^{2-}). From the above, it can be argued that the origin of calcium in the groundwater from the Rif (EM_7 and ES), Pre-Rif (EM_3), and Middle Atlas (EM_5 and EM_6) is mainly linked to the dissolution of carbonate rocks.

EM_2 and EM_4 are also close to the line but with very low concentrations. This can be explained if the contribution of Ca^{2+} from the alkaline granite came from amphiboles and the calcium part of plagioclases with a sodium tendency.

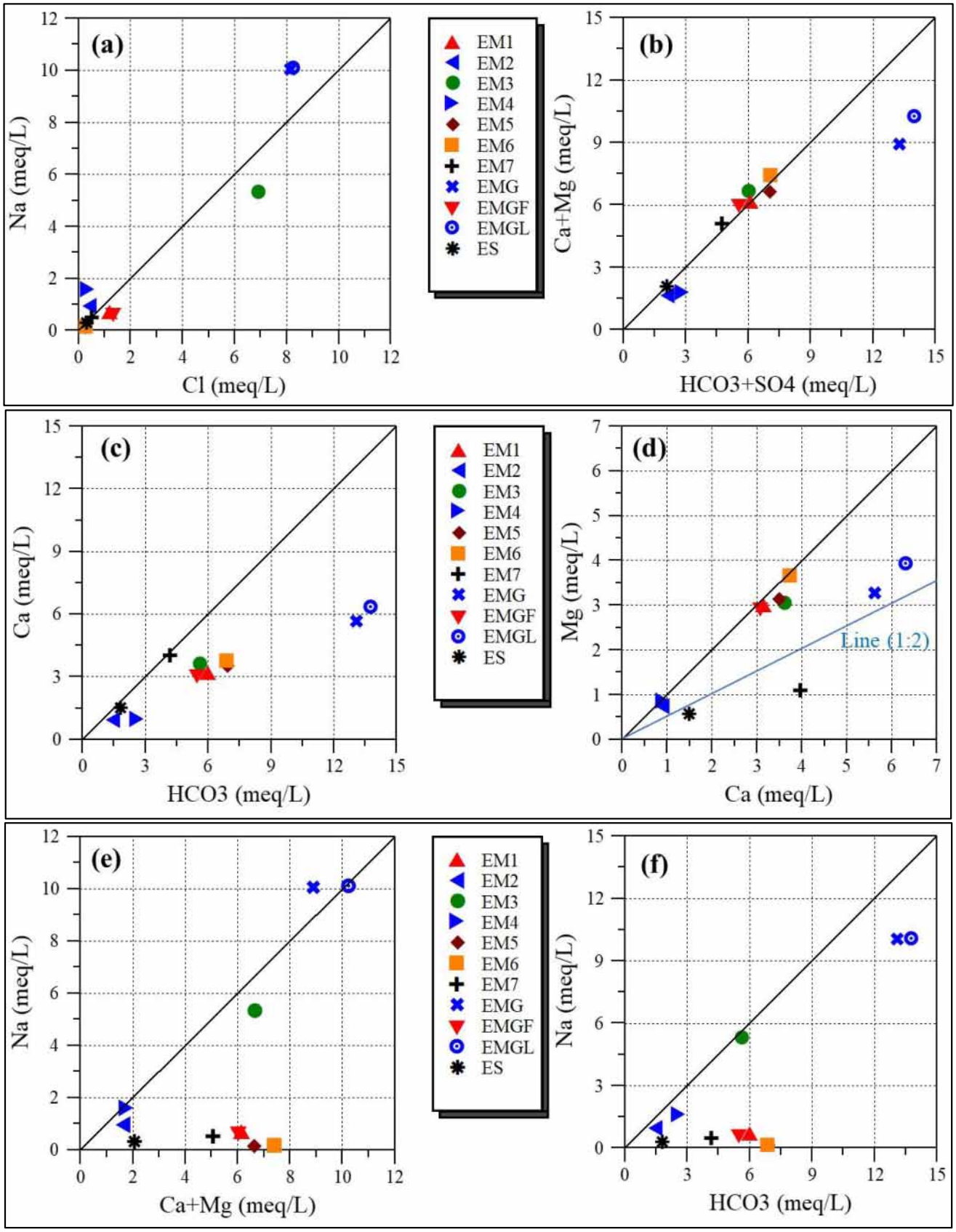

Figure 4. Binary correlation plots between different parameters. (**a**) Na vs. Cl; (**b**) (Ca + Mg) vs. (HCO_3 + SO_4); (**c**) Ca vs. HCO_3; (**d**) Mg vs. Ca; (**e**) Na vs. (Ca + Mg); (**f**) Na vs. HCO

The correlation diagram between the Na^+ and (Ca^{2+}+Mg^{2+}) (Figure 4e) shows a high concentration of sodium ions in the waters coming from the plateau of Oulmes and the thermal water of the Pre-Rif (EM_3). This concentration is almost equal to the concentration of divalent cations. The Na^+/HCO_3^- ratio of these waters is close to 1 (Figure 4f).

For the waters originating from the Oulmes plateau, the enrichment in sodium ion compared to chlorides and the predominance of bicarbonates in the salt load compared to divalent cations favor the process of alteration of alkaline-type granite silicates by hydrolysis as the origin of chemism [43]. In an alkaline context, the alteration of silicates enriches the water with sodium and bicarbonates [44].

Hydrothermal alteration, which is known to occur in EM_G and EM_{GL}, can also further enrich these waters in sodium ions [45]. For EM_3, the Na^+ ions can also come from the evaporate layers present in the Miocene detrital marls of the Pre-Rif, which explains its chlorinated and non-carbonated facies.

3.2.2. Ion Exchange Index

The cation exchange between water and clays is one of the important processes responsible for the evolution of groundwater during its transit through the reservoir. However, Ca^{2+} and Mg^{2+} can be exchanged mainly with the Na^+ ion. In addition, the Garcia diagram showing the relationship between (Ca^{2+}+Mg^{2+})-(SO_4^{2-}+HCO_3^-) and (Na^++K^+-Cl^-) was also used to test for cation exchange. Cation exchange occurs in the aquifers if the ratio between (Ca^{2+}+Mg^{2+})-(SO_4^{2-}+HCO_3^-) and (Na^++K^+-Cl^-) is about −1 [46]. In the absence of this exchange, all analytical points should lie close to the origin [47] (Figure 5).

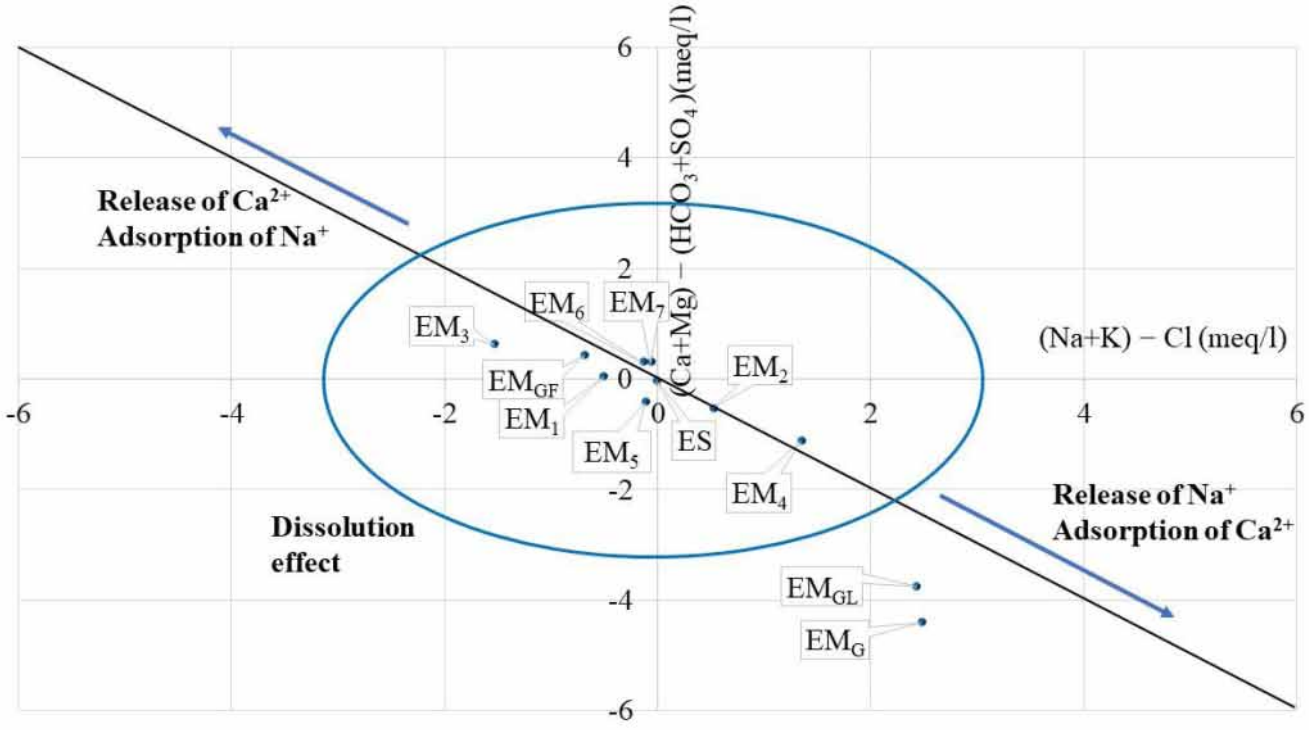

Figure 5. Scatter plot of ((Ca+Mg) − (HCO_3+SO_4)) versus ((Na+K) − Cl

The results of the samples in the cation exchange diagram (Figure 5), show that most of the samples are influenced by the dissolution effect (the analytical points should lie close to the origin), except for carbogazeous natural mineral water from the Oulmes plateau (EM_G and EM_{GL}), which is out of the dissolution effect zone the, which could suggest that the chemical composition of these waters is controlled by the direct-ion exchange process in relation to enrichment in sodium ions by direct ion exchange with altered zones

of granite rich in phyllosilicates or clays. However, the points could be on or close to the line characterized by a slope of −1, then possibly another process such as the hydrolysis of alkaline feldspars must be involved in the sodium excess found in these waters.

Another equation system, the chloro-alkaline ratios, CAI-1 and CAI-2, allows us to determine the exchange processes between water and rocks for (Na^++K^+) and (Ca^{2+}+Mg^{2+}).

$$\text{CAI-1} = \frac{Cl^- - \left(Na^+ + K^+\right)}{Cl^-}$$

$$\text{CAI-2} = \frac{Cl^- - \left(Na^+ + K^+\right)}{\left(SO_4^{2-} + HCO_3^- + CO_3^{2-} + NO_3^-\right)}$$

- CAI close to 0: there is a balance between the chemical compositions of the water and the aquifer.
- CAI < 0: the aquifer releases calcium and magnesium and fixes sodium and potassium, direct exchange.
- CAI > 0: the aquifer releases sodium and potassium and fixes calcium and magnesium, indirect exchange.

Figure 6 presents the two ion exchange indices (CAI-1 and CAI-2) calculated for the different mineral and spring waters. We note that the sign and the value of the indices strongly depend on the origin of the waters.

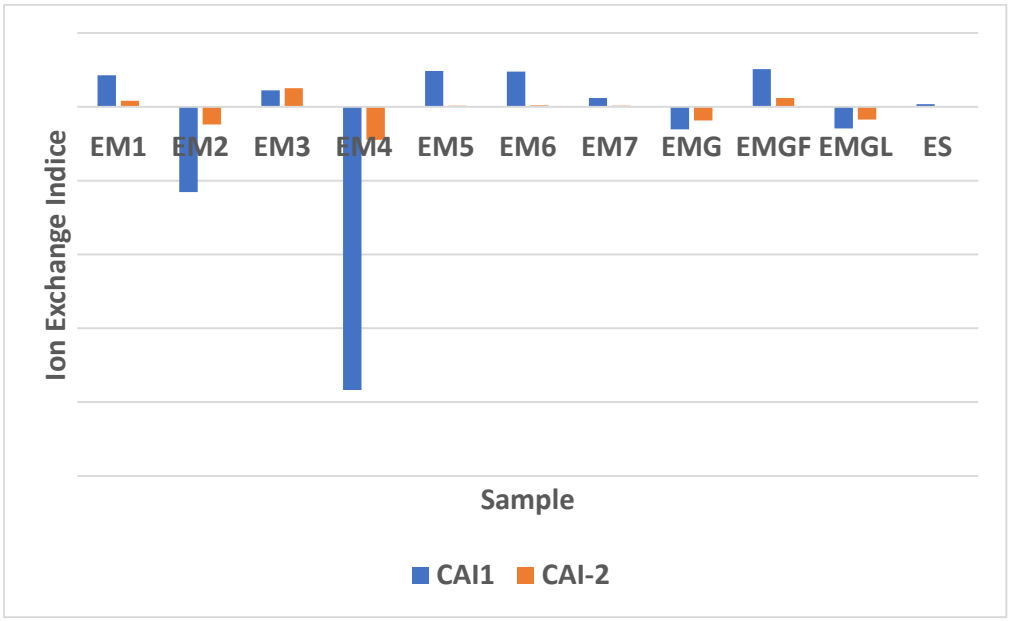

Figure 6. Ion exchange indices.

The samples of water coming from the Middle Atlas and Rif present positive indexes, they underwent exchanges of the indirect base. For these waters, the HCO_3^- concentrations are higher than those of the alkaline earths, which indicates that these waters are softened by base exchange (Figure 6).

The waters coming from the Oulmes plateau have negative indexes, they are in chloro-alkaline imbalance. Samples of the original bottled waters from the Oulmes plateau (EM_2, EM_4, EM_G, and EM_{GL}) show a higher alkaline earth concentration than HCO_3^-, which indicates that these waters have been hardened by the direct exchange.

However, the indexes are globally close to 0 or low, and the main process, as shown previously in Figure 5, is a chemical equilibrium process that dominates. Concerning EM_G and EM_{GL}, the ion exchange index is very low and confirms that the exchange process is

not the main explanation to highlight the sodium excess, the hydrolysis of felspars seems more suitable.

3.2.3. Saturation Index

To confirm the dissolution/precipitation process of some main minerals, calcite, dolomite halite, and gypsum, the saturation index for all samples was calculated using Phreeqc V.3.7.3 software.

$$SI = \log IAP/K$$

With IAP: ion activity product and K: mineral solubility constant.

SI = 0 determines an equilibrium state of the mineral in the water, SI < 0 is an undersaturated state, and SI > 0 is an oversaturated state.

Figure 7 shows the results of the saturation index obtained for all the samples studied. All the samples show a saturation index clearly below the equilibrium line (undersaturation) for halite and gypsum considering the weak concentration of the associated ions. The saturation index for dolomite and calcite show undersaturation or close to saturation, except for EM5 and EM6, which are oversaturated in calcite and dolomite and allow for a possible precipitation of these minerals. In fact, the range −0.5/0.5 represents an unstable condition and it is not so obvious to determine the real chemical conditions.

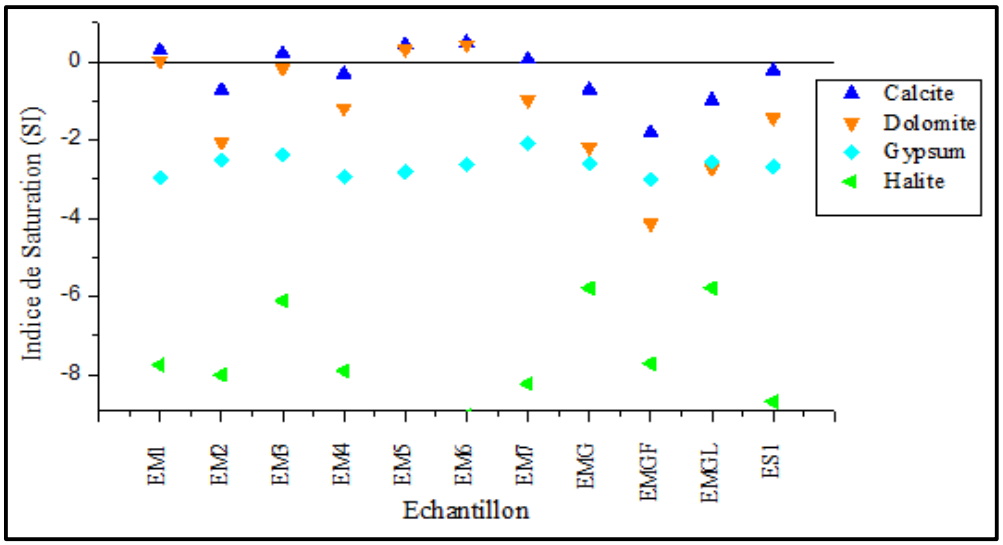

Figure 7. Saturation indices of the different minerals for each sample.

3.2.4. Gibbs Diagram

In order to confirm the results obtained previously concerning the origin of the mineralization of bottled waters in Morocco, we used the Gibbs diagram, which is widely used by researchers [48] and allows us to define the main trends which control the water mineralization origin.

The projection of the results on the Gibbs diagram (Figure 8) shows that all the waters studied are mainly influenced by the phenomenon of water–rock interaction. This implies that the water–rock interaction is the most important natural factor determining the chemistry of all-natural mineral water by recharge from surface water.

3.3. Isotopic Characterization

3.3.1. Relation between $\delta^{18}O$ and $\delta^{2}H$ in Rainwater and Water Sources

Two series of $\delta^{18}O$ and $\delta^{2}H$ isotope analyses were carried out in 2015 and 2018 on the water from the bottles studied (except ES_1 measured in 2015 only). The oxygen-18 ($\delta^{18}O$ in ‰ vs. V-SMOW) and deuterium ($\delta^{2}H$ in ‰ vs. V-SMOW) contents of bottled water in Morocco are presented in Table 4.

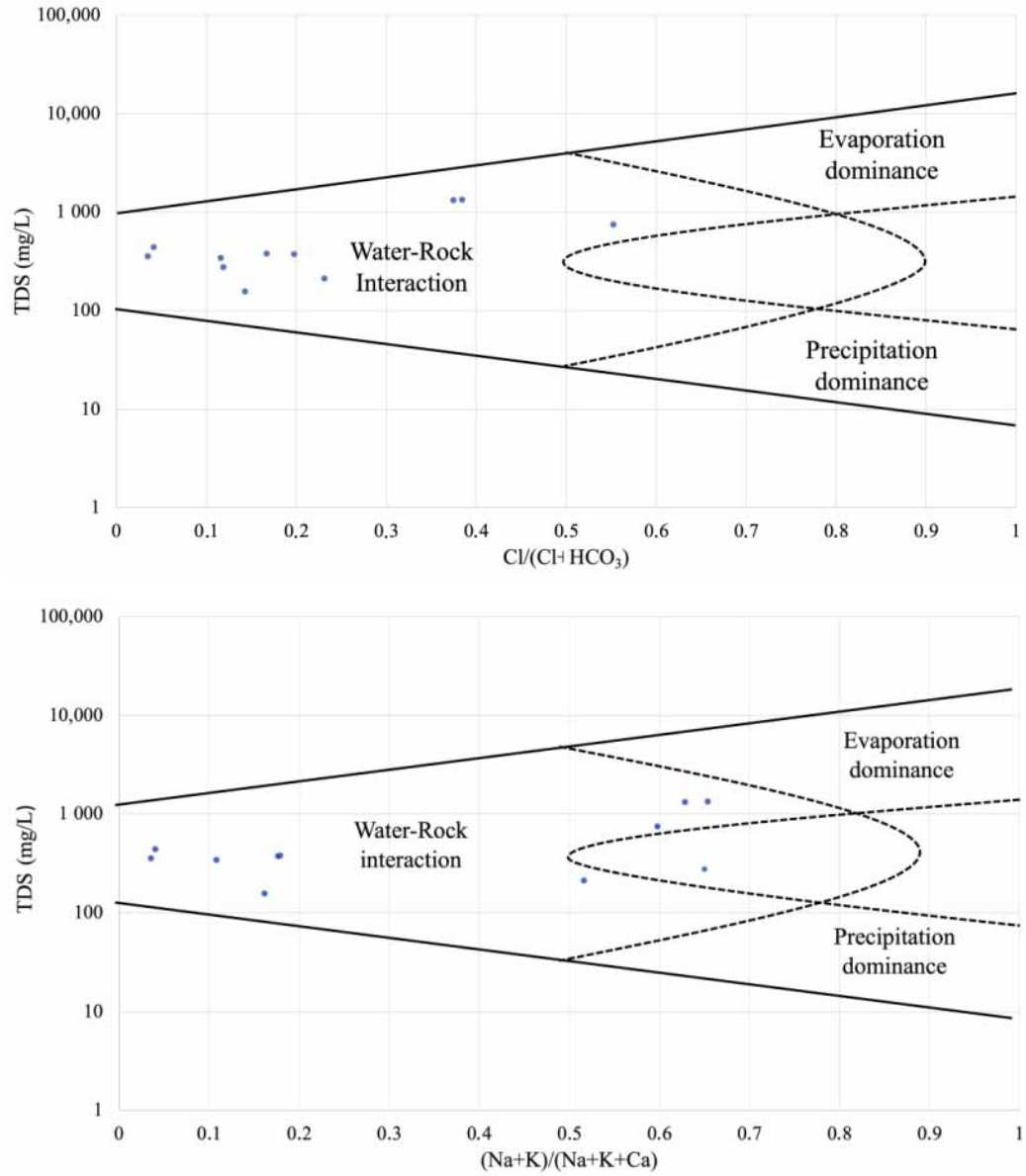

Figure 8. Gibbs diagram.

Table 4. Composition in $\delta^{18}O$ and $\delta^{2}H$ in 2015 and 2018.

	$\delta^{18}O$ (‰)	$\delta^{2}H$ (‰)	d-Excess (‰)	$\delta^{18}O$ (‰)	$\delta^{2}H$ (‰)	d-Excess (‰)	Origin
		2015			2018		
EM_1	−6.67	−42.5	10.8	−6.93	−41.4	14.1	Middle Atlas
EM_2	−6.30	−37.6	12.8	−6.61	−37.9	15.0	Oulmes
EM_3	−6.49	−42.2	9.7	−6.79	−41.4	12.9	Middle Atlas
EM_4	−5.98	−36.9	10.9	−6.30	−37.7	12.7	Oulmes
EM_5	−7.63	−45.4	15.6	−7.74	−45.4	16.5	Middle Atlas
EM_6	−6.92	−45.2	10.2	−7.27	−45.0	13.2	Middle Atlas
EM_7	−5.35	−30.4	12.3	−5.57	−34.6	10.0	Rif
EM_G	−6.89	−38.9	16.3	−7.20	−38.3	19.3	Oulmes
EM_{GF}	−6.93	−42.6	12.9	−6.93	−41.4	14.1	Middle Atlas
EM_{GL}	−6.87	−38.1	16.9	−7.09	−36.6	20.1	Oulmes
ES_1	−5.35	−30.4	12.3				Rif

The oxygen-18 and deuterium isotopic data in 2015 and 2018 were generally rather stable (Table S3), which shows that these aquifers are large enough to allow good mixing of successive annual recharges. The variability on the d-excess was slightly greater, from 2‰ to 3‰ in amplitude, partly explained by the fact that the analytical errors on the two isotopes are cumulative. The values in deuterium excess (d-excess), ranged from +8 to +16‰ for the waters analyzed in 2015 and from +11 to +20‰ for those of 2018.

Based on the 2015 results, the waters sampled in the Middle Atlas (EM_1, EM_3, EM_6), those from the Oulmes plateau (EM_4), and those from the Rif (EM_7, ES) showed a mixed footprint in terms of origin, air masses with a mixture of rain from the Atlantic, where d-excess is close to 10, and Mediterranean origin, where d-excess >10 (Table 4). The depleted isotopic content of EM_5 is to be linked with its elevation, which is the highest (Table 5), and the strong excess of deuterium is for its part also linked to the altitude. As for carbogazeous natural mineral water, the high values of d-excess may be the consequence of tectonic structures responsible for the ascent of deeper water [49]. For the waters of the Rif region located on the Mediterranean coast and more exposed to Mediterranean rains, the d-excess is greater than +12‰.

Table 5. Altitude and $\delta^{18}O$ results of the samples.

Water Type	$\delta^{18}O$ (‰) (2015)	$\delta^{18}O$ (‰) (2018)	Altitude (m asl)
EM_1	−6.67	−6.93	247
EM_2	−6.30	−6.61	1108
EM_3	−6.49	−6.79	245
EM_4	−5.98	−6.3	934
EM_5	−7.63	−7.74	1560
EM_6	−6.92	−7.27	1360
EM_7	−5.35	−5.57	402
EM_G	−6.89	−7.20	1050
EM_{GF}	−6.93	−6.93	247
EM_{GL}	−6.87	−7.09	1050
ES	−5.35		314

To better understand the cycles of the groundwater extracted to fill the bottles, we compared our isotopic analysis results to the analyses of rainwater at a monthly scale taken in the Pre-Rif (Fez-Saiss) between 1994 and 2018 by the Directorate of National Meteorology within the framework of the GNIP network of the IAEA, Rabat. The number of paired analyses for $\delta^{18}O$ and $\delta^{2}H$ in the database is 115, which was reduced to 91 after eliminating the rains whose d-excess showed an evaporation mark probably linked to sub-cloud evaporation of small amounts of rainfall. Figure 9 plots these results with a calculated linear equation $\delta^{2}H = 7.73\ \delta^{18}O + 11.9$ ($R^2 = 0.945$ and a weighted mean of −5.25‰ for oxygen-18 and −28.5‰ for deuterium (GNIP database, https://www-naweb.iaea.org/napc/ih/IHS_resources_isohis.html (accessed on 15 June 2022). This line is called the local meteoric water line (LMWL) and it is determined by the GNIP database. Between 1994 and 2015, it was slightly above the global meteoric water line (GMWL) ($\delta^{2}H = 8\ \delta^{18}O + 10$), determined by Craig [50] for the first time, and confirmed by numerous studies including Cidu and Bahaj [28]. It is below the Mediterranean meteoric water line (MMWL) of equation $\delta^{2}H = 8\delta^{18}O + 22$‰ corresponding to the rainfall of eastern Mediterranean regions [51]. The Fez-Saiss line is between the global line and the west Mediterranean line defined by Celle-Jeanton et al. [52] in the south of France, which shows a d-excess of 13,7‰, and a d-excess of 13,9‰ in the north of Tunisia [53], showing a stronger imprint of the Atlantic rains in the study area.

Three distinct meteorological groups fall along the Fès-Saiss line [16] that are a result of (1) rains of Atlantic origin with a d-excess close to 10‰, (2) rains of Mediterranean origin marked by a d-excess greater than 12‰, and (3) rains that reach higher values of d-excess up to 25‰, which occurs when masses of humid Atlantic or Mediterranean air come up through the Sahara, drying up before precipitating on coastal areas. In Morocco,

the rainwater d-excess shows well-defined seasonal variations with maxima during winter months, associated with depleted $\delta^{18}O$ values. The d-excess minima (associated with enriched $\delta^{18}O$ values) observed in the summer are due to weak and rare rainfall with high evaporation rates. In the region of Fez-Saiss, the rains are mainly of Mediterranean origin or come up from the Sahara (60% of d-excess> 12‰), and 40% are of Atlantic or mixed origin.

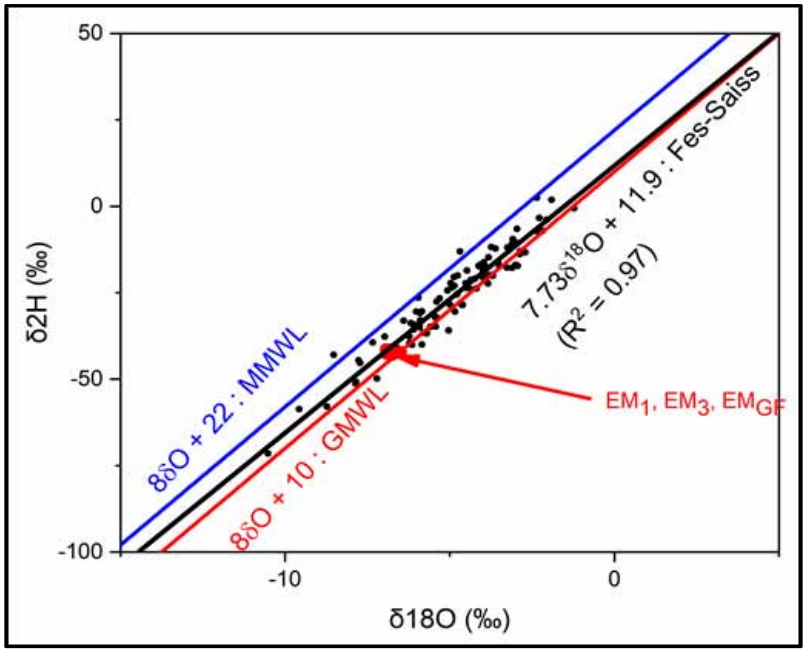

Figure 9. Local meteoric water line corresponding to the Middle Atlas (Fez-Saiss).

The line of equation ($\delta^2H = 7.73\delta^{18}O + 11.9$; $R^2 = 0.97$) for the rains of Fez-Saiss in the Middle Atlas is different from the line relating to the rainwater in the Anti Atlas [54], ($\delta^2H = 8\delta^{18}O + 14.5$), in the High Atlas ($\delta^2H = 8\delta^{18}O + 13.5$) [55], and in central Morocco ($\delta^2H = 8\delta^{18}O + 13.0$) [56]. The data from the previous works come from short time series (2 years), which could be statistically biased with respect to the Fez-Saiss series.

In Figure 9 we have plotted the points that correspond to water from the Middle Atlas area (EM_1, EM_{GF}, and EM_3). These points represent bottled groundwater and plot close to the heart of the rainfall point cluster. This result confirms the stability of the isotope footprint which has not changed over the timeframe investigated in stable and deep aquifers. Indeed, Figure 10 gives the positions of the different bottled waters in Morocco in the isotopic composition diagram (δ^2H, $\delta^{18}O$). We note that the positioning of the different groups remained unchanged around the LMWL in 2015 and 2018, which indicates that the isotopic composition of the groundwater sampled was not significantly modified during the production process.

The waters are divided into five subgroups according to their altitude and their gaseous or flat nature (Figure 10). Subgroup 1 represents the lowest isotopic values, indicating that these waters have either infiltrated during a previous colder or rainier climatic regime or that this corresponds to the highest recharge zones (altitude >1500 m), which is more likely (Table 5). The oxygen and hydrogen isotope compositions of these water samples (EM_5 and EM_6) are significantly lower than those of other samples. They are bottled in the Middle Atlas (Ben Smim and Ain Soltane), which reaches altitudes of 1600 and 1400 m, respectively, with the highest depleting water in δ^2H and $\delta^{18}O$ caused by the altitude effect.

Subgroups 2 and 3 are mineral waters from Fez-Saiss and Oulmes, respectively. The position of these samples relative to the local meteoric water line (LMWL: $\delta^2H = 7.73\delta^{18}O + 11.9$) is close to group 5 (carbogazeous natural mineral waters).

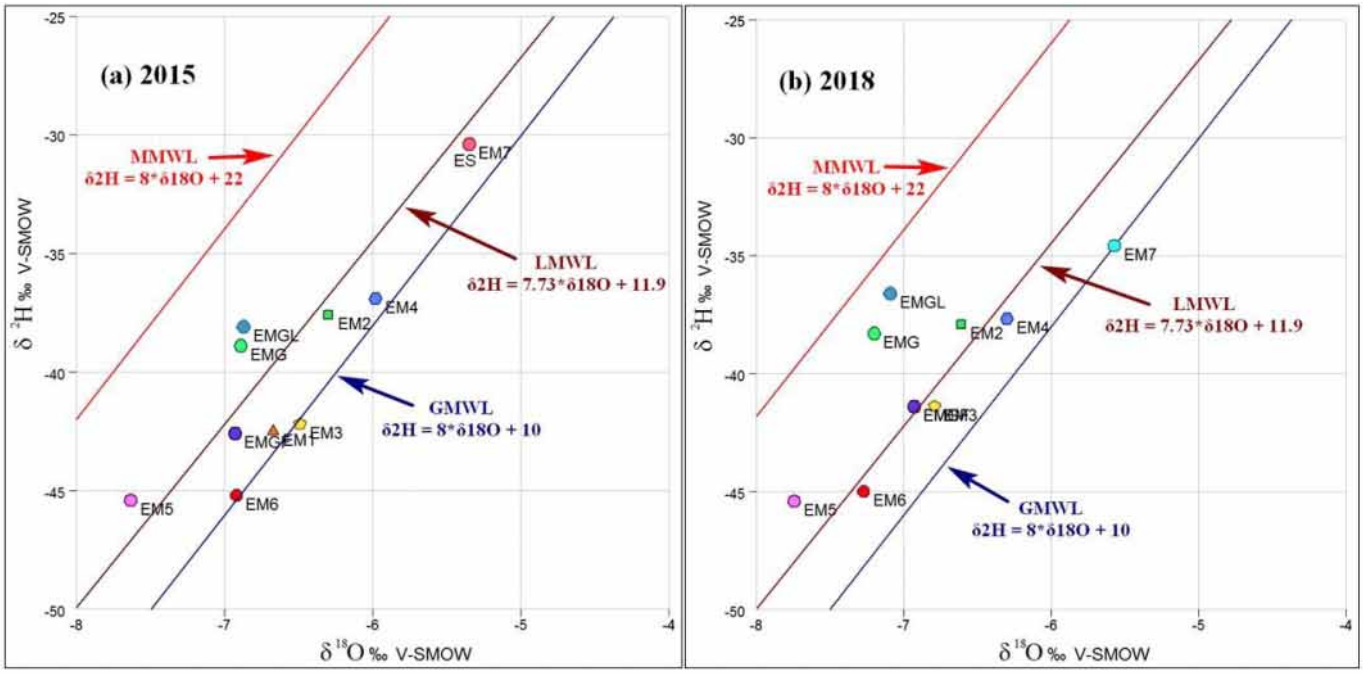

Figure 10. Relationship between δ^2H and $\delta^{18}O$ in 2015 and 2018. MMWL: mediterranean meteoric water line; LMWL: local meteoric water line; GMWL: global meteoric water line.

Subgroup 4 represents waters from the Rif (EM_7 and ES). These waters, taken from a low altitude in an area close to the Mediterranean coast, are the least loaded with heavy isotopes.

Subgroup 5 includes naturally carbonated or carbonated mineral waters EM_G, EM_{GL}, and EM_{GF}. EM_{GF} water, of the same geographical origin as EM_1, is slightly offset from EM_1 in 2015, showing that the gasification process could cause a slight isotopic fractionation., however, in 2018 they present the same values in oxygen-18 or deuterium. Oulmes thermal carbogazeous natural mineral waters (EM_G and EM_{GL}), from the same geographic region as EM_2, exhibit an isotopic ratio shifted from the LMWL line, which may be due to the presence of CO_2. For the carbonated waters of Lalla Haya of Oulmes (EM_G), the presence of deep CO_2, whose origin comes from magmatic degassing of the waters, could have caused a depletion of about 1‰ in $\delta^{18}O$ and enrichment in deuterium [57].

3.3.2. Correlation between Altitude and $\delta^{18}O$

Determining the altitudes and recharge areas of sources is essential for the management of groundwater resources. Recharge altitudes can be estimated from stable isotope contents, the isotopic signal of the local recharge is generally being a function of the local annual atmospheric temperature at the surface [58].

We sought to determine the relationship that may exist between the isotope ratio of $\delta^{18}O$ and the infiltration altitude of surface water. Table 5 and Figure 11 give the values of $\delta^{18}O$ and the altitudes of the different groundwater production sites.

Figure 11 shows the correlation between $\delta^{18}O$ values obtained in 2015 and in 2018, as a function of the altitude. The isotopic altitudinal gradient in Morocco has been estimated at −0.27‰ per 100 m of elevation [59] and −0.25‰ per 100 m in the Middle Atlas, the Rif, and the city of Fes [60]. For reference, we have drawn on the same graph the two lines, −0.27‰ and −0.25‰. We note that most still mineral waters are positioned along the two lines. However, the waters from the Pre-Rif area (EM_1, EM_{GF}, and EM_3), located in the region of Fez at an altitude of 250 m, are well below the line. The production units are located in a zone situated between the Middle Atlas and the Rif, two reliefs of high elevation. The

recharge of these sources is therefore probably done at a higher altitude in the Middle Atlas or the Rif, around a mean elevation of 1200 m according to the isotopic gradient.

The waters of the Rif, which are being extracted at the foot of the limestone ridge mountain, would appear to recharge at an altitude of around 700 m if the same gradient can be applied. The carbonated waters of Oulmes are below the regional altimeter lines consistently with the presence of CO_2, which depletes the water in $\delta^{18}O$.

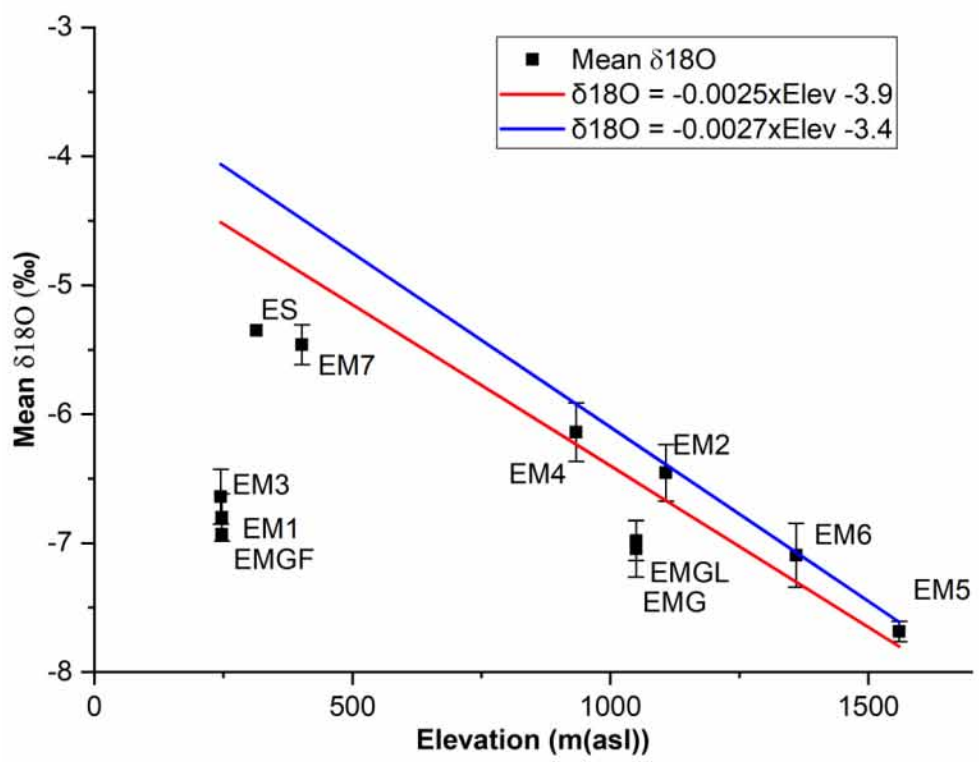

Figure 11. Relationship between the altitude and water $\delta^{18}O$ values. Blue line: the isotopic altitudinal gradient of Morocco; red line: the isotopic altitudinal gradient of the Middle Atlas.

4. Conclusions

The physicochemical parameters and the stable isotope data of the 11 brands of mineral water bottled and marketed in Morocco have provided information on the origin and the mechanisms of the mineralization of these waters.

Geological formations are the main factors controlling the hydrochemical evolution of groundwater. While the original waters of Oulmes (granite and schist) show Na-HCO_3 water types, the Middle Atlas and Rif waters are of the Ca-HCO_3 type due to their interaction with carbonate and limestone rocks. The waters of the Middle Atlas are of the Ca-HCO_3 type linked to the emergence of sources in the carbonaceous Jurassic, which is chiefly limestones and dolomites, and of the Na-Cl type for EM_3 in relation to the detrital Miocene marls of the Pre-Rif deposited on the Jurassic carbonates of the Atlas. Regarding trace elements, the waters originating from the Oulmes plateau have very high levels of K, Si, Li, Rb, Sr, and Cs, in connection with their high concentration in granite rocks.

The local meteoric line of the region of Fez-Sais in the Middle Atlas is different from that of the regions further south of Morocco. In the Middle Atlas, there is a stronger imprint from the Atlantic rains. The stable isotope values ($\delta^{18}O$ and $\delta^{2}H$) of the 11 samples lie along the local and global meteoric water lines and are unaffected by evaporation. The distribution of the isotopic composition of the waters subjected to a local recharge process is local (all waters except EM_1, EM_{GF}, and EM_3), is consistent with the regional altitudinal isotopic gradient reported earlier, between −0.25‰/100 m and −0.27‰/100 m for oxygen-18. The waters from the Pre-Rif area (EM_1, EM_{GF}, and EM_3), located in the region of Fez at an altitude of 250 m, are clearly below the line and show a recharge process at higher altitudes,

around 1000 m. Mineral waters are divided into five subgroups according to their altitude and their gaseous or still nature. The combination of the use of groundwater chemistry and stable isotopes can improve our understanding of the geochemical acquisition processes of groundwater and help determine its recharge zone in mountainous areas.

Supplementary Materials: The following supporting information can be downloaded at: https://www.mdpi.com/article/10.3390/geosciences13020038/s1, Table S1. Date of production and analysis of the different types of water.

Author Contributions: M.G. wrote the main manuscript text, prepared figures, and performed the calculations; E.G. wrote the main manuscript text; J.-D.T. wrote the main manuscript text; M.B. wrote the main manuscript text; N.P. wrote the main manuscript text. All authors reviewed the manuscript. All authors have read and agreed to the published version of the manuscript.

Funding: This research received no specific grant from any funding agency in the public, commercial, or not-for-profit sectors.

Data Availability Statement: No datasets were generated or analyzed during the current study.

Conflicts of Interest: The authors declare no conflict of interest.

References

1. Ochilova, N.R.; Muratova, G.S.; Karshieva, D.R. The Importance of Water Quality and Quantity in Strengthening the Health and Living Conditions of the Population. *CAJMS* **2021**, *2*, 399–402.
2. Official Bulletin. *n°6506 du 6 Octobre 2016 Dahir n°1-16-113 du 6 Kaada 1437 Portant Promulgation de la loi n°36-15 Relative à L'eau*; Nabu Press: Charleston, South Carolina, 2016.
3. EU Directive 1980/777/EEC. Council Directive 1980/778/EEC of 15 July 1980 on the Approximation of the Laws of the Member States Relating to the Exploitation and Marketing of Natural Mineral Water. *Off. J. Eur. Communities* **1980**, *L229*, 1–10.
4. EU Directive 1996/70/EC. Directive 1996/70/EC of the European Parliament and of the Council of 28 October 1996 amending Council Directive 80/777/EEC on the approximation of the laws of the Member States relating to the exploitation and marketing of natural mineral waters. *Off. J. Eur. Communities* **1996**, *L299*, 26–28.
5. EU Directive 2003/40/EC. Establishing the list, concentration limits and labelling requirements for the constituents of natural mineral waters and the conditions for using ozone-enriched air for the treatment of natural mineral waters and spring waters. *Off. J. Eur. Communities L* **2003**, *126*, 34–39.
6. Grappein, B.; Lasagna, M.; Capodaglio, P.; Caselle, C.; Luca, D.A.D. Hydrochemical and Isotopic Applications in the Western Aosta Valley (Italy) for Sustainable Groundwater Management. *Sustainability* **2021**, *13*, 487. [CrossRef]
7. Mushtaq, N.; Younas, A.; Mashiatullah, A.; Javed, T.; Ahmad, A.; Farooqi, A. Hydrogeochemical and isotopic evaluation of groundwater with elevated arsenic in alkaline aquifers in Eastern Punjab, Pakistan. *Chemosphere* **2018**, *200*, 576–586. [CrossRef]
8. Bouaissa, M.; Ghalit, M.; Taupin, J.D.; El Khattabi, J.; Gharibi, E. Assessment of groundwater quality in the Bokoya Massif (Central Rif, Northern Morocco) using several analytical techniques. *Euro-Mediterr. J. Env. Integr.* **2021**, *6*, 1–11. [CrossRef]
9. Bouaissa, M.; Gharibi, E.; Ghalit, M.; Taupin, J.D.; El Khattabi, J. Identifying the origin of groundwater salinization in the Bokoya massif (central Rif, northern Morocco) using hydrogeochemical and isotopic tools. *Groundw. Sustain. Dev.* **2021**, *14*, 100646. [CrossRef]
10. Fugedi, U.; Kuti, L.; Jordan, G.; Kerek, B. Investigation of the hydrogeochemistry of some bottled mineral waters in Hungary. *J. Geochem. Explor.* **2010**, *107*, 305–316. [CrossRef]
11. Bouaissa, M.; Ghalit, M.; Taupin, J.D.; Patris, N.; El Khattabi, J.; Gharibi, E. Assessment of medium mountain groundwater for consumption and irrigation using quality index method: Application to the Bokoya Massif (Central Rif, Northern Morocco). *Arab. J. Geosci.* **2021**, *14*, 1–13. [CrossRef]
12. Voica, C.; Cristea, G.; Feher, I. Multielement and Isotopic Characterization of Bottled Mineral Waters on the Romanian Market. In *Bottled and Packaged Water vol. 4: The Sciences of Beverages*; Woodhead Publishing: Cambridge, UK, 2019; pp. 121–144.
13. Clark, I.D.; Fritz, P. *Environmental Isotopes in Hydrogeology*; CRC Press: Boca Raton, FL, USA, 2013.
14. Qin, W.; Han, D.; Song, X.; Liu, S. Environmental isotopes ($\delta^{18}O$, $\delta^{2}H$, ^{222}Rn) and hydrochemical evidence for understanding rainfall-surface water-groundwater transformations in a polluted karst area. *J. Hydrol* **2021**, *592*, 125748. [CrossRef]
15. Li, J.; Pang, Z.; Kong, Y.; Wang, S.; Bai, G.; Zhao, H.; Yang, Z. Groundwater isotopes biased toward heavy rainfall events and implications on the local meteoric water line. *J. Geophys. Res. Atmos* **2018**, *123*, 6259–6266. [CrossRef]
16. Gourcy, L. Isotopic composition of precipitation in the Mediterranean basin in relation to air circulation patterns and climate. *Iaea-Tecdoc* **2005**, *1453*, 223.
17. Felipe-Sotelo, M.; Henshall-Bell, E.R.; Evans, N.D.M.; Read, D. Comparison of the chemical composition of British and Continental European bottled waters by multivariate analysis. *J. Food Compost. Anal.* **2015**, *39*, 33–42. [CrossRef]

18. Peters, M.; Guo, Q.; Strauss, H.; Zhu, G. Geochemical and multiple stable isotope (N, O, S) investigation on tap and bottled water from Beijing, China. *J. Geochem. Explor.* **2015**, *157*, 36–51. [CrossRef]
19. Bertoldi, D.; Bontempo, L.; Larcher, R.; Nicolini, G.; Voerkelius, S.; Lorenz, G.D.; Brereton, P. Survey of the chemical composition of 571 European bottled mineral waters. *J. Food Compos. Anal.* **2011**, *24*, 376–385. [CrossRef]
20. Dinelli, E.; Lima, A.; De Vivo, B.; Albanese, S.; Cicchella, D.; Valera, P. Hydrogeochemical analysis on Italian bottled mineral waters: Effects of geology. *J. Geochem. Explor.* **2010**, *107*, 317–335. [CrossRef]
21. Hssaisoune, M.; Bouchaou, L.; Sifeddine, A.; Bouimetarhan, I.; Chehbouni, A. Moroccan Groundwater Resources and Evolution with Global Climate Changes. *Geosciences* **2020**, *10*, 81. [CrossRef]
22. Frizon de Lamotte, D.; Crespo-Blanc, A.; Saint-Bezar, B.; Comas, M.; Fernadez, M.; Zeyen, H.; Ayarza, H.; Robert-Charrue, C.; Chalouan, A.; Zizi, M.; et al. *The Transmed Atlas—The Mediterranean Region from Crust to Mantle, Cavazza, W., Roure, F., Spakman, W., Stampfli, G., Ziegler, P., Eds.*; Springer: Berlin, Germany, 2004.
23. Elbatloussi, D.; Cheddadi, M.; Dadi, S.; Ruthy, I.; Orban, P.; Dassargues, A. *Carte Hydrogéologique du Plateau d'Oulmès (Maroc)*; Notice Explicative, 2005. Available online: https://orbi.uliege.be/bitstream/2268/127371/2/NOTICEp_carte_hydro_oulmes.pdf (accessed on 15 May 2022).
24. Heron, D.P.; Ghienne, J.F.; El Houicha, M.; Khoukhi, Y.; Rubino, J.L. Maximum extent of ice sheets in Morocco during the Late Ordovician glaciation. *Palaeogeogr. Palaeoclimatol. Palaeoecol* **2007**, *245*, 200–226. [CrossRef]
25. Cherai, B.; Idrissi, B.E.F.; Charroud, M.; El Hnot, H. Les mouvements de terrain dans le secteur urbain de la ville de Fès (Maroc): Facteurs de genèse et cartographie des zones à risques. *AJIRAS* **2017**, *5*, 405–414.
26. Sabri, K.; Marrero-Diaz, R.; Ntarmouchant, A.; dos Santos, T.B.; Ribeiro, M.L.; Solá, A.R.; Jesus, A.P. Geology and hydrogeochemistry of the thermo-mineral waters of the South Rif Thrust (Northern Morocco). *Geothermics* **2019**, *78*, 28–49. [CrossRef]
27. Charroud, M.; Cherai, B.; Benabdelhadi, M.; Falguères, C. Impact de la néotectonique quaternaire sur la dynamique sédimentaire du Saïs (Maroc): Du bassin d'avant fosse pliocène au plateau continental quaternaire. *Quaternaire Revue de l'Association Française Pour l'étude du Quaternaire* **2007**, *18*, 327–334. [CrossRef]
28. Cidu, R.; Bahaj, S. Geochemistry of thermal waters from Morocco. *Geothermics* **2000**, *29*, 407–430. [CrossRef]
29. Saadi, M.; Hilali, E.A.; Bensaıd, M.; Boudda, A.; Dahmani, M. Geological map of Morocco, scale 1: 1000000. *Edition du Service Géologique du Maroc. Notes et Mémoires* **1985**, *8*, 260.
30. Chalouan, A.; Michard, A.; El Kadiri, K.; Negro, F.; de Lamotte, D.F.; Soto, J.I.; Saddiqi, O. The Rif Belt. In *Continental Evolution: The Geology of Morocco*; Springer: Berlin/Heidelberg, Germany, 2008; pp. 203–302.
31. Baird, R.B.; Eaton, A.D.; Rice, E.W. *Standard Methods for the Examination of Water and Wastewater*, 23rd ed.; American Public Health Association, American Water Works Association, and Water Environment Federation: Washington, DC, USA, 2017.
32. WHO. Guidelines for drinking-water quality. *WHO Chron.* **2011**, *38*, 104–108.
33. Official Bulletin n°6506 of October 6, 2016 Dahir n°1-16-113 of 6 Kaada 1437 Promulgating Law n°36-15 Relating to Water. 2016. Available online: http://www.auks.ma/wp-content/uploads/2019/11/loi%20eau.pdf(accessed on 27 November 2022).
34. Mimi, A.L.; Dhia, H.B.; Bouri, S.; Lahrach, A.; Abidate, L.B.; Bouchareb-Haouchim, F.Z. Application of chemical geothermometers to thermal springs of the Maghreb, North Africa. *Geothermics* **1998**, *27*, 211–233. [CrossRef]
35. Zarhloule, Y.; Bouri, S.; Lahrach, A.; Boughriba, M.; El Mandour, A.; Ben Dhia, H. Hydrostratigraphical study, geochemistry of thermal springs, shallow and deep geothermal exploration in Morocco: Hydrogeothermal potentialities. In Proceedings of the World Geothermal Congress, Antalya, Turkey, 24–29 April 2005; pp. 24–29.
36. Barkaoui, A.E.; Zarhloule, Y.; Rimi, A.; Verdoya, M.; Bouri, S. Hydrogeochemical investigations of thermal waters in the northeastern part of Morocco. *Environ. Earth Sci.* **2014**, *71*, 1767–1780. [CrossRef]
37. Reimann, C.; Birke, M. *Geochemistry of European Bottled Water*; Borntraeger Science Publishers: Stuttgart, Germany, 2010.
38. Rossiter, A.G.; Gray, M.C. Barium contents of granites: Key to understanding crustal architecture in the southern Lachlan Fold Belt? *Aust. J. Earth Sci.* **2008**, *55*, 433–448. [CrossRef]
39. Shin, W.J.; Ryu, J.S.; Shin, H.S.; Jung, Y.Y.; Ko, K.S.; Lee, K.S. Major and Trace Element Geochemistry of Korean Bottled Waters. *Water* **2020**, *12*, 2585. [CrossRef]
40. Petrović, T.; Mandić, M.Z.; Veljković, N.; Papić, P.; Stojković, J. Geochemistry of Bottled Waters of Serbia. In *Clean Soil and Safe Water*; Springer: Dordrecht, The Netherlands, 2012; pp. 247–266.
41. Piper, A.M. A graphic procedure in the geochemical interpretation of water-analyses. *Eos Trans. AGU* **1944**, *25*, 914–928. [CrossRef]
42. Schoeller, H. Qualitative evaluation of groundwater resources. In *Methods and Techniques of Groundwater Investigations and Development*; UNESCO: Paris, France, 1967; pp. 44–52.
43. Velde, B. *Introduction to Clay Minerals: Chemistry, Origins, Uses and Environmental Significance*; Chapman & Hall: London, UK, 1992; Volume 198.
44. Elango, L.; Kannan, R. Rock–water interaction and its control on chemical composition of groundwater. *Dev. Environ. Sci.* **2007**, *5*, 229–243.
45. Taillefer, A. Interactions Entre Tectonique et Hydrothermalisme: Rôle de la Faille Normale de la Têt sur la Circulation Hydrothermale et la Distribution des Sources Thermales des Pyrénées Orientales. Ph. D. Thesis, Université Montpellier, Montpellier, France, 2017.
46. Garcia, G.M.; Hidalgo, M.D.V.; Blesa, M.A. Geochemistry of groundwater in the alluvial plain of Tucuman province, Argentina. *Hydrogeol. J.* **2001**, *9*, 597–610. [CrossRef]

47. McLean, W.; Jankowski, J.; Lavitt, N. Groundwater quality and sustainability in an alluvial aquifer, Australia. In *Groundwater: Past Achievements and Future Challenges*; A.A. Balkema: Rotterdam, The Netherlands, 2000; pp. 567–573.
48. Mohamed, A.; Asmoay, A.; Alshehri, F.; Abdelrady, A.; Othman, A. Hydro-geochemical applications and multivariate analysis to assess the water–rock interaction in arid environments. *Appl. Sci.* **2022**, *12*, 6340. [CrossRef]
49. Paternoster, M.; Liotta, M.; Favara, R. Stable isotope ratios in meteoric recharge and groundwater at Mt. Vulture volcano, southern Italy. *J. Hydrol.* **2008**, *348*, 87–97. [CrossRef]
50. Craig, H. Isotopic variations in meteoric waters. *Science* **1961**, *133*, 1702–1703. [CrossRef] [PubMed]
51. Nir, A. Development of isotope methods applied to groundwater hydrology. *Isot. Tech. Hydrol. Cycle* **1967**, *11*, 109–116.
52. Celle-Jeanton, H.; Travi, Y.; Blavoux, B. Isotopic typology of the precipitation in the Western Mediterranean Region at three different time scales. *Geophys. Res. Lett. Am. Geophys. Union* **2001**, *28*, 1215–1218. [CrossRef]
53. Ben Ammar, S.; Taupin, J.-D.; Ben Alaya, M.; Zouari, K.; Patris, N.; Khouatmia, M. Using isotopes and geochemistry tools to characterize groundwater in a coastal phreatic aquifer from the NE of Tunisia: Guenniche basin. *J. Arid. Environ.* **2020**, *178*, 104150. [CrossRef]
54. Ettayfi, N.; Bouchaou, L.; Michelot, J.L.; Tagma, T.; Warner, N.; Boutaleb, S.; Vengosh, A. Geochemical and isotopic (oxygen, hydrogen, carbon, strontium) constraints for the origin, salinity, and residence time of groundwater from a carbonate aquifer in the Western Anti-Atlas Mountains, Morocco. *J. Hydrol.* **2012**, *438*, 97–111. [CrossRef]
55. Ait Lemkademe, A.; Michelot, J.L.; Benkaddour, A.; Hanich, L.; Maliki, A. Isotopic and hydrochemical approach to the functioning of an aquifer system in the region of Marrakech (Morocco). *Rapid Commun. Mass Spectrom.* **2011**, *25*, 2785–2792. [CrossRef]
56. Ouda, B.; El Hamdaoui, A.; Ibn Majah, M. Isotopic composition of precipitation at three Moroccan stations influenced by oceanic and Mediterranean air masses. In *Isotopic Composition of Precipitation in the Mediterranean Basin in Relation to Air Circulation Patterns and Climate*; IAEA-Tecdoc 1453: Vienna, Austria, 2005; pp. 125–140.
57. Olive, P.; Dassargues, A.; Griere, O.; Ruthy, I.; El Youbi, A. Caractérisation Isotopique des eaux du Granite et de l'auréole Métamorphique d'Oulmès (Maroc Central). *In GIRE3D, Integrated Water Resources management and Challenges of the Sustainable Development*. 2006. Available online: https://orbi.uliege.be/bitstream/2268/3459/1/publi135-2006.pdf (accessed on 15 May 2022).
58. Gat, J.R. The isotopes of hydrogen and oxygen in precipitation. In *Handbook of Environmental Isotope Geochemistry*; IAEA: Vienna, Austria, 1980; Volume 1.
59. Sefrioui, S.; Fassi Fihri, O.; El Ouali, A.; Marah, H.; Newman, B.; Essahlaoui, A. Utilisation des outils isotopiques pour la détermination de l'altitude de recharge des principales sources du bassin de Sebou-Maroc. *J. Geomaghreb.* **2010**, 6.
60. Winckel, A.; Marlin, C.; Dever, L.; Morel, J.L.; Morabiti, K.; Makhlouf, M.B.; Chalouan, A. Apport des isotopes stables dans l'estimation des altitudes de recharge de sources thermales du Maroc. *C.R. Geosci.* **2002**, *334*, 469–474. [CrossRef]

Disclaimer/Publisher's Note: The statements, opinions and data contained in all publications are solely those of the individual author(s) and contributor(s) and not of MDPI and/or the editor(s). MDPI and/or the editor(s) disclaim responsibility for any injury to people or property resulting from any ideas, methods, instructions or products referred to in the content.